CONF-900520--1
EGG-M-89488

MEASUREMENT OF AIR ENTRAINMENT IN PLASMA JETS

J. R. Fincke, R. Rodriquez, C. G. Pentecost
Idaho National Engineering Laboratory
EG&G Idaho, Inc., Idaho Falls, ID

EGG-M--89488

DE91 001943

ABSTRACT

The concentration and temperature of air entrained into argon and helium plasma jets has been measured using coherent anti-Stokes Raman spectroscopy (CARS). The argon plasma flow field is characterized by a short region of well behaved laminar flow near the nozzle exit followed by an abrupt transition to turbulence. Once the transition to turbulence occurs, air is rapidly mixed into the jet core. The location of the transition region is determined by the rapid cooling of the jet and the resulting increase in Reynolds number. In contrast, the helium plasma flow field never exceeds a Reynolds number of 200 and remains laminar. The entrainment process in this case is controlled by molecular diffusion rather than turbulent mixing.

INTRODUCTION

In the plasma spray fabrication of coatings the composition of the surroundings into which the plasma jet flows is known to exert considerable influence on the behavior of the jet and can alter the characteristics and quality of the coatings produced [1-3]. The goal of the work described here is to examine the fundamentals of entrainment mechanisms for both laminar and turbulent plasma jets. As an initial step in understanding this process we have applied the technique of coherent anti-Stokes Raman spectroscopy (CARS) to the measurement of concentration and temperature in plasma jet flow fields. The CARS technique is applicable to the measurement of the concentration and temperature of any Raman active species, including the common atmospheric gases O_2, N_2, CO, and CO_2. In the work described here we have chosen N_2 as the species to be probed. The CARS spectra of N_2 is well known and the dissociation and ionization characteristics result in non-depleted populations of neutral, molecular nitrogen at temperatures in excess of 6000 K. The initial results on argon and helium plasmas, issuing into a stagnant atmospheric pressure air environment, are presented here.

MEASUREMENT TECHNIQUE

Non-intrusive optical diagnostic techniques such as CARS have become standard tools in high temperature flow-field research. CARS has the

advantage of high conversion efficiency, a laser-like coherent signal beam for high collection efficiency, excellent fluorescence and luminosity discrimination, and high spatial and temporal resolution. The theory of CARS and its application as a combustion diagnostic tool has been detailed in several reviews [4-6]. A CARS signal, Figure 1, is generated when two laser beams at frequency w_1, (termed the pump beams) and one laser beam at frequency w_2 (termed the Stokes beam) interact through the third-order nonlinear susceptibility of the medium $X^{(3)}$ to generate an oscillating polarization and thus coherent (laser like) radiation at frequency $w_3=2w_1-w_2$. The intensity of the CARS signal, I_3, is proportional to:

$$I_3 \propto I_1^2 I_2 (3X^{(3)})^2$$

where I_i is the intensity at frequency w_i. This relation assumes that the required momentum phase matching is satisfied and that both beams have the same focal diameter. The third-order nonlinear susceptibility, $X^{(3)}$, which governs CARS can be expressed as:

$$X^{(3)}=X_n+X_r$$

where X_n is the nonresonant contribution and X_r is the Raman resonant contribution. The nonresonant susceptibility is proportional to the number density of the species present, and is generally a slowly varying function of wavelength. The resonant contribution, far from electronic resonance, is given by:

$$X^{(3)}=(2c^4/hw^2)\ N\ \Sigma[\sigma\Delta(v,j)/(w_r-(w_1-w_2)-iG_{v,j})]$$

where N is the number density of the species probed; $\Delta(v,j)$ is the population difference between the states involved in the Raman Transition; σ is the Raman scattering cross section; w_r is the frequency of a Raman active rotational or vibrational state; and $G_{v,j}$ is the Raman half-width. When the frequency difference (w_1-w_2) is close to the

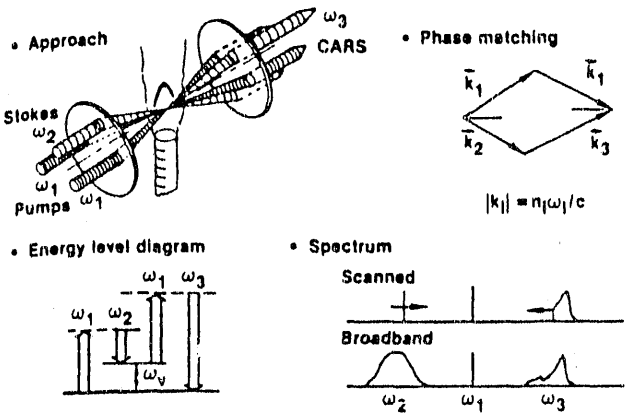

Figure 1. Coherent anti-Stokes Raman spectroscopy.

frequency of a Raman resonance of a species, w_r, the magnitude of the CARS radiation at w_3 is resonantly enhanced, resulting in a signature unique to that molecular species.

CARS spectra can be acquired in two basic ways, Figure 1. The scanned approach uses a spectrally-narrow Stokes beam to generate one small segment of the CARS spectrum. The Stokes beam is then scanned across the Raman frequency range to generate a high-resolution CARS spectrum. This method requires considerable time and is limited to temporally stationary flow fields. The broadband approach employs a Stokes source that has a broad spectrum (150-200 cm^{-1}). This allows the entire CARS spectrum to be generated simultaneously, on the time scale of the laser pulse. High spatial resolution is achieved by using a crossed beam geometry [6]. The CARS spectrometer consists of a frequency-doubled, Q-switched Nd:YAG laser. The second-harmonic green beam is used both as a pump beam for the dye laser which generates the Stokes beam, and as the CARS pump beam. The general beam geometry is shown in Figure 1. The focusing lenses are 100 mm focal length, resulting in a ellipsoidal measurement volume approximately 200 μm in diameter by 1.5 mm in length. In generating the spatial dependence of concentration and temperature, the plasma torch is moved relative to the stationary CARS measurement volume.

Temperatures are derived from the spectral distribution of the CARS signal and concentration is derived from the strength of the signal. In the work performed here, a quick-fit technique [7], based on the full-width at half maximum of the spectral signal, has been used to derive temperatures from spectral data. The temperature determination is calibrated against a platinum, platinum-rhodium thermocouple, while the concentration measurement is calibrated by varying the concentration of air mixed into a cold argon jet. A correction to the measured concentration is derived by assuming vibrational equilibrium and calculating a Boltzmann correction factor using the measured temperature. Alternately, spectral fitting procedures such as the CARSFT [8] computer code, or similar technique may be used to derive the same information from data acquired. The uncertainties in the concentration and temperature measurements are estimated to be 6 and 8 percent respectively.

RESULTS

The test conditions are summarized in Table I. The free flow region of the plasma jet issued in to stagnant laboratory air at an atmospheric pressure of 86 kPa. The argon gas flow rate is 0.59 SCMH and the helium gas flow rate is 0.61 SCMH. The nozzle exit diameter 1.27 cm for the argon case and 0.95 cm diameter for the helium results.

Table I. Operating conditions

gas	current	voltage	efficiency	power deposited
Ar	250 a	20 v	26 %	1.30 kW
He	350 a	30 v	6 %	.63 kW

A shadowgraph of the resulting argon jet appears in Figure 2. The argon jet flow field is characterized by a short region of well behaved laminar flow near the nozzle exit followed by an abrupt transition to turbulence. The turbulence is initially confined to the shear region between the laminar flow exiting the nozzle and the cold surroundings. The laminar region can easily be lengthened by several centimeters by increasing the power input to the torch [9]. The location of the transition region is determined by the rapid cooling of the jet and the resulting increase in Reynolds number. The estimated Reynolds number at the torch exit is approximately 100, based on the nozzle diameter. At the location of the transition to turbulence the Reynolds number is on the order of 10,000. Once turbulence is initiated air is rapidily mixed into the core flow by an engulfment process. Turbulent eddies are formed in the region of large shear on the boundary between the jet and the surrounding air. As these eddies are pulled downstream by the jet flow they roll up and engulf large quantities of air, which is then convected into the core region of the jet. In contrast, the helium jet, Figure 3, has a Reynolds number of approximately 30 at the exit of the nozzle, increasing to a value of approximately 200 as the jet cools. The low value of Reynolds number inhibits transition and the flow field remains laminar.

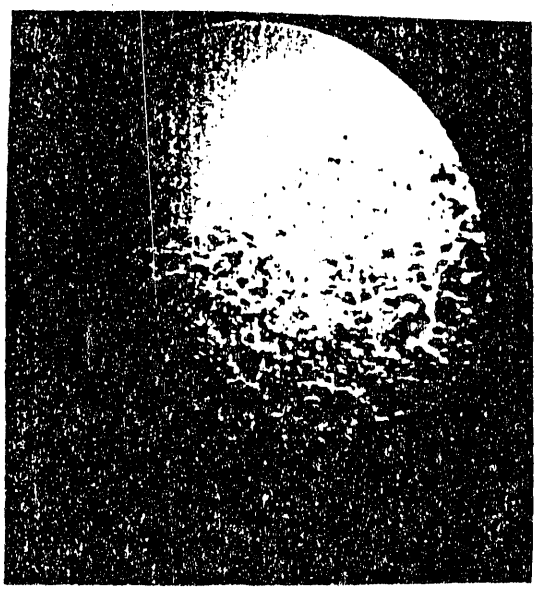

Figure 2. Shadowgraph of argon plasma jet.

Figure 3. Photograph of helium plasma jet.

Contour plots of temperature and relative concentration appear in Figures 4 and 5 for the argon and helium cases respectively. The relative concentration is normalized by the number density of N_2 at ambient conditions, $N_0 \approx 1.7e19$. The rapid entrainment of air into the core flow of the jet coincident with the onset of turbulence and jet breakup is evident in the argon concentration contours. This transition region is not as pronounced in the associated temperature field. The helium results on the other hand, show a persistence of the laminar, all helium core flow for many nozzle diameters. The entrainment mechanism is driven by molecular diffusion rather than turbulent mixing.

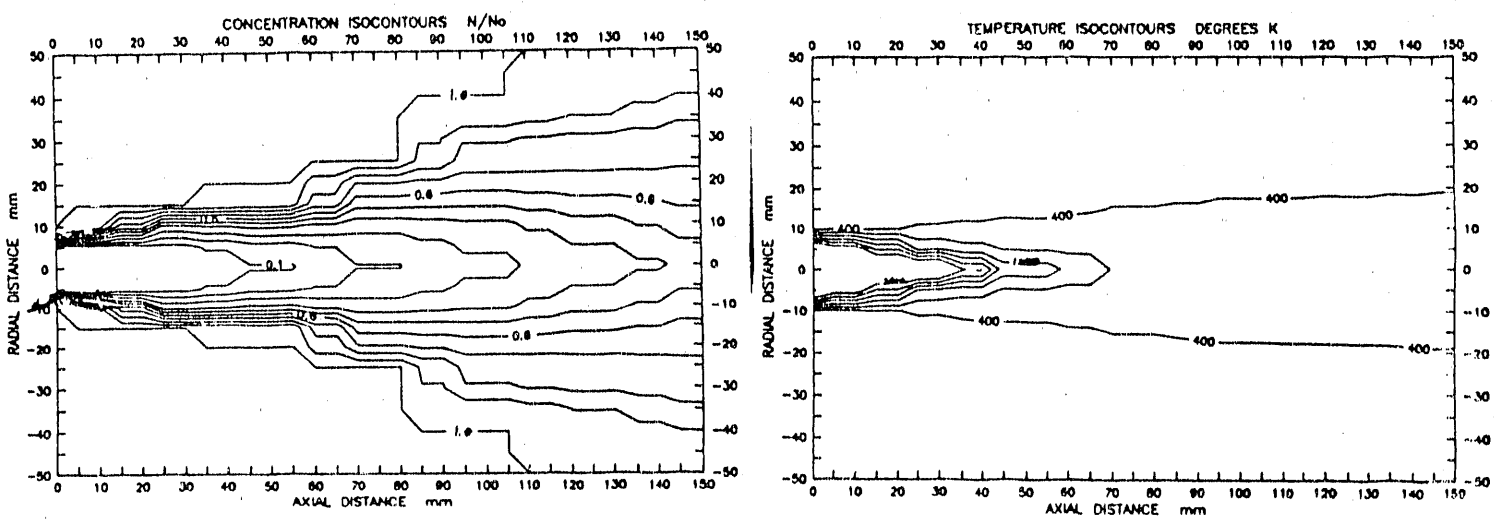

Figure 4. Contour plots of nitrogen concentration and temperature for argon plasma jet.

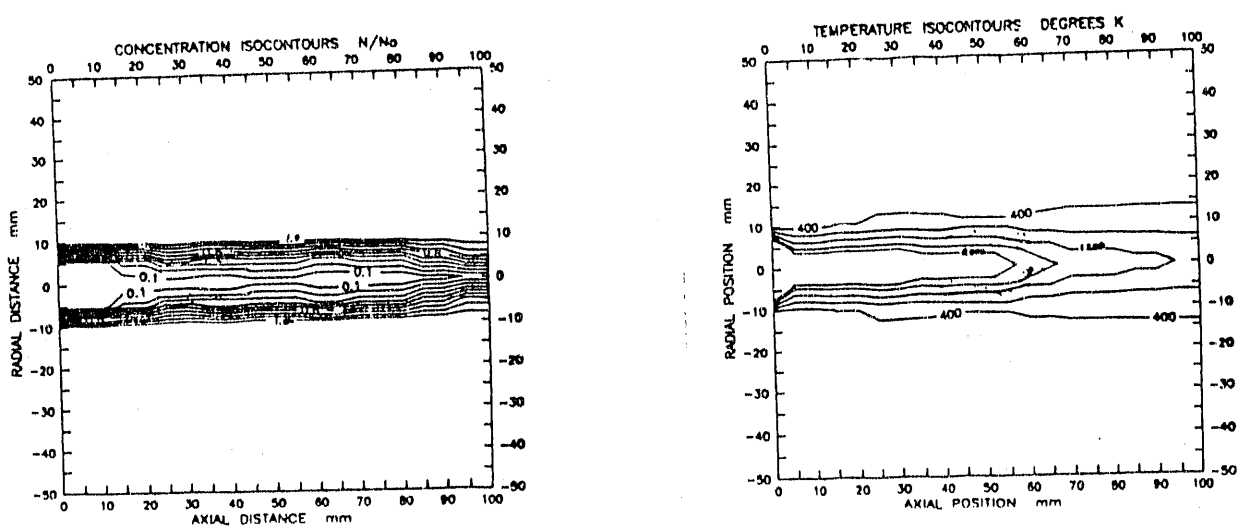

Figure 5. Contour plots of nitrogen concentration and temperature for helium plasma jet.

CONCLUSIONS

The CARS technique has been sucessfully applied to the measurement of N_2 temperature and entrainment in argon and helium plasma jets issuing into stagnant air environments. The entrainment process in the argon jet, under the conditions tested, was found to be characterized by an initial laminar region followed by the rapid onset of turbulence and jet breakup. The location of the transition is dependent on the Reynolds number, which is determined primarily by the temperature field. Once turbulence appears the air is rapidly entrained into the jet core. The physical properties of helium, on the other hand, are such that the Reynolds number remains small (<200) and the jet remains laminar. The entrainment process in the helium jet is controlled by molecular diffusion.

ACKNOWLEDGMENT

This work was supported by the U. S. Department of Energy, Office of Energy Research, Office of Basic Energy Sciences, U.S. Department of Energy under Contract No. DE-AC07-76ID01570.

REFERENCES

1. Vardelle, M., Vardelle, A., Roumilhac, Ph., and Fauchais, P., Proceedings of the National Thermal Spray Conference, Cincinnati, OH, pp. 177-121, October 1988.
2. Vinayo, M. E., Kassabji, F., Guyonnet, J.,and Fauchais, P., J. Vacuum Science Technology, vol. 6, pp. 2483-2489, 1985.
3. Varacalle, D., J., et al, Symposium Volume of the 1989 TMS/ASM Northeast Regional Meeting, May 1989.
4. Levenson, M. D., Introduction to Nonlinear Laser Spectroscopy, Academic Press, New York, 1982.
5. Antcliff, R. R. and Jarrett, O., Review of Scientific Instrumentation, vol. 58, pp. 2075-2080.
6. Eckbreth, A. C. and Anderson, T. J., Applied Optics, vol. 24, pp. 2731-2736,1985.
7. Eckbreth, A. C., Dobbs, G. M., Stufflebeam, J. H., and Tellex, P. A., Applied Optics, Vol. 23, pp. 1328-1339, 1984.
8. Palmer, R. E, SAND89-8206, Sandia National Laboratories, 1989.
9. Fincke, J. R., Rodriquez, R., and Pentecost, C. G., to be published in Plasma Processing and Synthesis of Materials, Materials Research Society Proceedings, San Francisco, CA, April 1990.

-END-

DATE FILMED

11/29/90